Dalton Transactions

PAPER

View Article Online
View Journal | View Issue

Cite this: *Dalton Trans.*, 2018, **47**, 10702

Highly luminescent lanthanide complexes sensitised by tertiary amide-linked carbostyril antennae†

Daniel Kovacs, Dulcie Phipps, Andreas Orthaber and K. Eszter Borbas *

Received 31st March 2018,
Accepted 12th June 2018

DOI: 10.1039/c8dt01270a

rsc.li/dalton

Carbostyrils are among the most widely used sensitising antennae for luminescent lanthanides; they afford bright complexes with Eu and Tb, and can also sensitise the emissions of the less commonly used Sm, Dy, Yb and Nd. Systematic studies on the effect of structural variations on the photophysical properties and lanthanide sensitising abilities of carbostyrils can therefore have a large impact. We replaced the secondary amide linker that connects the metal binding site to the antenna with a carboxymethyl-substituted tertiary amide. Eight Tb and Eu complexes were prepared. All had higher lanthanide luminescence quantum yields (Φ_{Ln}) than their secondary amide analogues; three Tb emitters had $\Phi_{Tb} > 40\%$. Eu complexes had Φ_{Eu} up to 11.6%. The antenna singlet and triplet excited states are slightly shifted, while the metal coordination sphere is unchanged by the introduction of the carboxymethyl group.

Introduction

Lanthanide (Ln)-based emitters occupy a unique niche among luminescent compounds. They have long emission lifetimes, narrow emission bands, are often highly photostable, and have negligible phototoxicities.[1–6] These properties are in sharp contrast to the rapid degradation, broad emission profiles and short lifetimes of organic emitters, or the toxicity of transition metal-based phosphorescent dyes or quantum dots. Ln(III) emission results from Laporte-forbidden f–f-transitions, and direct Ln(III) excitation is inefficient. Sensitisation by a light-harvesting antenna is common, and bypasses the small extinction coefficients of the Ln(III). Energy transfer (ET) from the antenna to the Ln can be efficient, and in the most successful cases, bright luminescent complexes are obtained.[2,7] The brightness of Ln(III) emitters ($B = \varepsilon \cdot \Phi$; ε: molar decadic absorption coefficient at λ_{ex}, Φ: dye's fluorescence quantum yield) depends on several factors, *e.g.* the number of absorbing and emitting units,[8–11] the efficiency of the antenna absorption and of the energy transfer,[12,13] the intrinsic quantum yield of the Ln(III), and the quenching processes that deplete the antenna and Ln(III) excited states.[14,15]

The development of new emitters is a lengthy and high-risk task. Therefore, there are substantial efforts directed towards the optimization of already reported luminescent Ln complexes, which encompass the understanding of the energy transfer mechanism and, if possible, elimination of quenching pathways. A well-known Ln excited state quenching pathway involves X–H overtones (X = O, N, C)[16,17] but can be avoided by the saturation of the Ln inner coordination sphere with a multidentate ligand, and, in some cases, by ligand deuteration.[18,19]

The quenching of the antenna excited state by atmospheric oxygen[21–23] and biologically relevant reductants has also been studied.[4,24,25] These quenching processes could be harnessed for the construction of responsive probes, or environmentally-activated Ln-based theranostics.[23,26–28]

Carbostyrils (quinolin-2(1*H*)-ones) are among the most widely used antennae for the sensitisation of Eu and Tb, of which the most commonly used one is cs124 (Scheme 1, **2a**).[29–37] Some are even effective for Sm and Dy,[38] as well as the near infrared (NIR) emitting Yb and Nd.[39] A variety of substituted carbostyrils have been reported (Fig. 1a).[38,40] Many were evaluated as antennae, even though in-depth photophysical characterizations are rare.[39] Most of the structural variations were limited to the peripheral substituents, usually in the 3 and 4 (R^1 and R^2, respectively in Fig. 1) positions. There are also a few examples of core *N*-substitutions (alkylations).[34] The effects of exocyclic *N*-alkylations on Ln sensitization have not been studied in detail, presumably because changes were expected to be small.

We hypothesised that the removal of the N–H bond may have a measurable effect on the Ln emission quantum yield, at

Department of Chemistry, Ångström Laboratory, Uppsala University, Box 523, 75120 Uppsala, Sweden. E-mail: eszter.borbas@kemi.uu.se

†Electronic supplementary information (ESI) available: NMR spectra and LC-MS traces for new compounds, and absorption, excitation and emission spectra of Ln complexes, crystallographic characterisation. CCDC 1832851 and 1833918. For ESI and crystallographic data in CIF or other electronic format see DOI: 10.1039/c8dt01270a

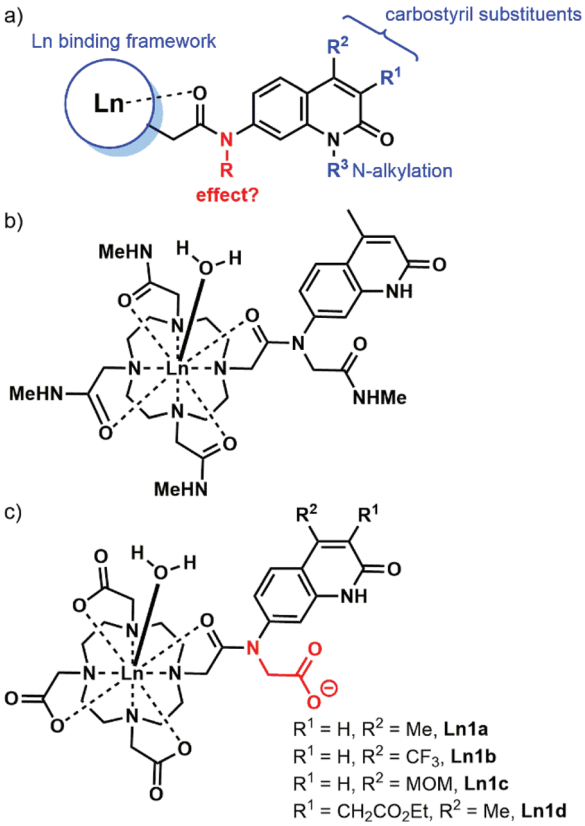

Fig. 1 (a) Common variations shown in blue in carbostyril-appended Ln complexes. (b) Eu complex reported by Parker and Williams in ref. 20. (c) Complexes studied here.

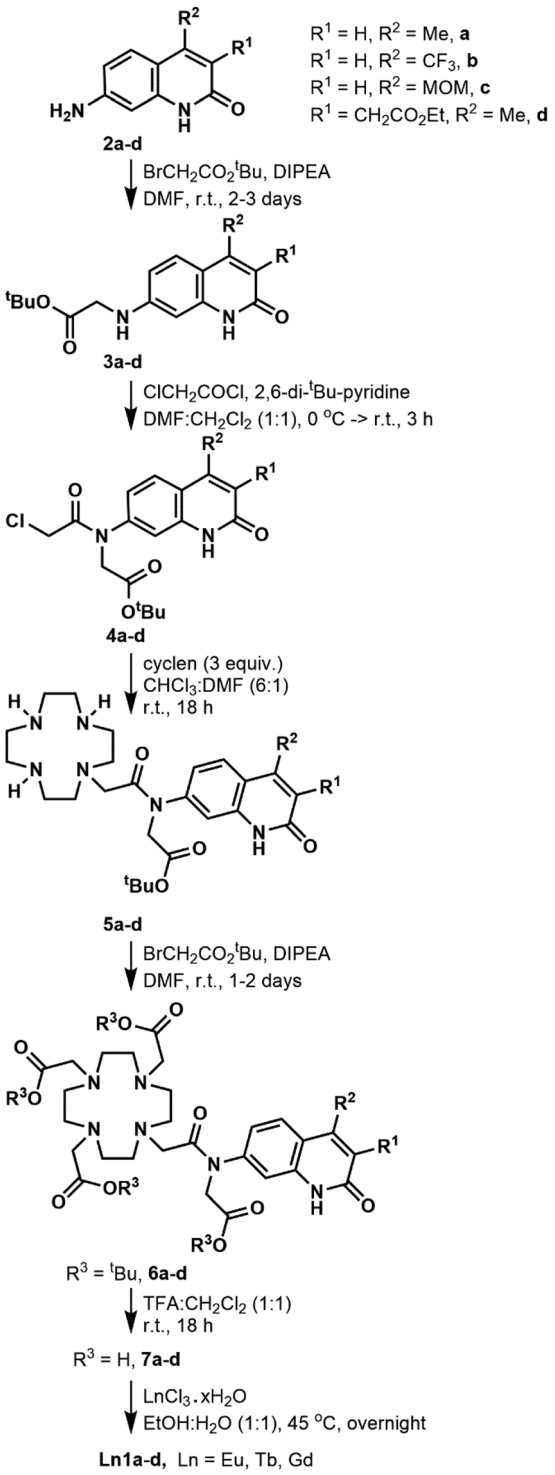

Scheme 1 Synthesis of the Ln complexes studied here.

least for the more sensitive Eu complexes. The majority of the reported carbostyril-appended Ln-emitters retain this N–H bond. Parker and Williams have prepared the tetraamide shown in Fig. 1b.[20] However, the methylamide arms bring further N–H oscillators into the proximity of the Ln. Furthermore, the +3 charge of this complex facilitates photo-induced electron transfer (PeT) from the excited antenna to the Eu by destabilizing Eu^{3+}. For most of the sensitised Eu(III) emitters, PeT quenches the luminescence.[41] Because of the combination of detrimental processes the evaluation of the contribution of the *N*-alkylation to the photophysics of the complex shown in Fig. 1b difficult. Here, we investigate the role of exocyclic *N*-alkylation in carbostyril-sensitised DO3A-type Ln complexes (Fig. 1c, DO3A = 1,4,7,10-tetraazacyclododecane-1,4,7-triacetic acid). Surprisingly, we found that *N*-alkylation with a carboxymethyl group afforded a dramatic increase in Ln emission for both Eu and Tb emitters. We attempt to explain these results based on spectroscopic and structural analyses.

Results and discussion

Synthesis

The DO3A-derived ligands were synthesised as shown in Scheme 1. For the Ln complex numbers see Fig. 1c. The general procedure was amenable to the preparation of all four ligands without significant adjustments in the protocols. Briefly, the carbostyrils **2a–d** were *N*-alkylated with *tert*-butyl bromoacetate in the presence of DIPEA. Acylation of secondary amines of **3a–d** was performed with 2,6-di-*tert*-butylpyridine

base. Other, less hindered and more nucleophilic bases (*e.g.* Et_3N) could not be used, as they got acylated by chloroacetyl chloride faster than the modestly nucleophilic carbostyril amines. The chloroacetylated derivatives **4a–d** were obtained in at least 72% yield after column chromatography on silica gel. Monoalkylation of cyclen yielded **5a–d** along with small amounts of di- and trialkylated side-products, which were readily removed upon purification. Less side-product was seen than in similar reactions of secondary amide carbostyrils, as due to the better solubilities of **4a–d** in $CHCl_3$ much less DMF co-solvent was needed, which improved the selectivity.

The secondary amines in **5a–d** were alkylated in DMF in the presence of DIPEA base. These conditions minimise the formation of the by-products that are *N*- or *O*-alkylated in the carbostyril core. The drawback of these conditions is that the DIPEA·HBr co-elutes with the product on silica gel in $CHCl_3$/acetone/MeOH systems. Therefore, the protected ligands **6a–c** required several chromatographic purification steps, and the purified products still contained varying amounts of DIPEA·HBr and DMF. For **6d** $CHCl_3$/acetone/EtOH eluent worked best, and an analytically pure sample was isolated after a single chromatographic step. However, a large amount of the product co-eluted with the DMF residues of the reaction mixture, which diminished the yield. Other bases (*e.g.* Na_2CO_3) afforded the *N*- or *O*-alkylated by-products. Finally, the *tert*-butyl esters were cleaved with a 1 : 1 mixture of CH_2Cl_2 and TFA. The reactions proceeded to completion overnight at room temperature, as shown by HPLC-analysis of the reaction mixtures. The ligands were isolated after column chromatography as white (**6a,c**) or yellow-white (**6b,d**) solids in at least 81% yield.

We have explored an alternative route to these ligands by reacting the known **8c**[39] with *tert*-butyl bromoacetate in acetonitrile at 70 °C in the presence of Na_2CO_3 (Scheme 2). After overnight reaction no carbostyril *N*-alkylation was observed either in the core or the exocyclic nitrogen. Longer reaction times yielded a mixture of **10c** and **13c**. Attempted alkylation of **5c** at 50 °C gave three observable products upon HPLC analysis of the reaction mixture. After their separation the major species was identified as **11c**. This sample was contaminated by approximately 5% of a product tentatively identified as **12c**, based on its HPLC-behaviour, mass spectrum and UV-Vis absorption spectrum. The desired product under these unoptimised conditions was isolated in 36% yield. Due to the observed overalkylations we did not pursue further this route.

Complexation with $EuCl_3$, $TbCl_3$ and $GdCl_3$ was carried out in EtOH : H_2O (1 : 1) mixture. The reaction was complete after 18 h according to HPLC-MS analysis of the reaction mixture. After completion, the crude products were isolated by extraction upon washing with Et_2O (dropwise addition of the reaction mixture to Et_2O). After layer separation, the aqueous phase was purified by column chromatography on silica gel. It was crucial to keep the stationary phase short. Elution from a longer column required the addition of aqueous ammonia to the eluent, which resulted in partial loss of the lanthanide ion.

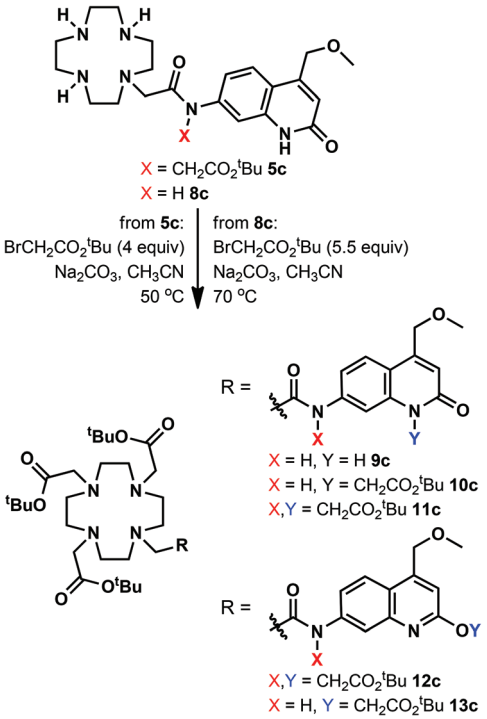

Scheme 2 Attempted alternative syntheses of the *N*-alkylated ligands.

Chemical characterisation

The identities of **2–7** were confirmed by ^1H and ^{13}C NMR spectroscopy and high resolution mass spectrometry (see ESI† for details). We were able to grow X-ray quality crystals from **5a** (Fig. 2, S1†). The cyclen moiety is disordered over two positions in the free ligand, which was modeled as a positional disorder without any geometric constraints of the two units. The site occupation factors are 0.592 and 0.408 for the major and the minor components, respectively.

The complexes were shown to be pure by HPLC-MS analysis (see ESI†). High resolution mass spectrometry (HR-MS) of the Ln complexes showed the deprotonated, singly negatively

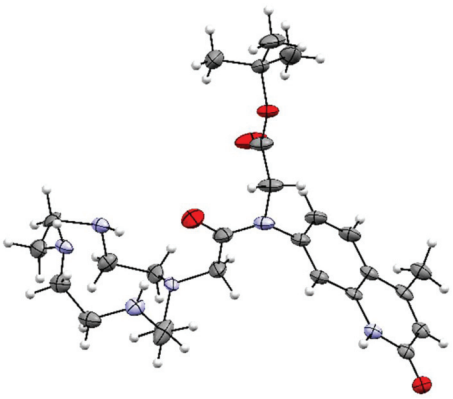

Fig. 2 Crystal structure of **5a**. Thermal ellipsoids are shown at the 30% (cyclen) probability levels. For clarity, only one of the disordered cyclen parts is shown.

charged molecule ions with the expected isotope distribution pattern. Further support for the identities of the metal complexes was provided by their photophysical properties (*vide infra*). Briefly, Eu and Tb complexes displayed the characteristic red and green Ln emissions, respectively, while Gd complexes only had antenna-based photophysical activities.

We could obtain crystals from a Dy complex of the non-*N*-alkylated analogue of the **1d** ligand (**Dy9d**, Fig. 3). This structure shows a different configuration of the antenna-linking amide compared to that found in the current ligands, which may impact the photophysical properties (*vide infra*). The Dy center shows a classical monocapped square antiprismatic arrangement typical of this type of complexes. The four carboxylic oxygen and four nitrogen atoms form two near ideal planes that are almost coplanar; the angle between the least square planes is only 0.63(8)°. One additional water molecule caps the face spanned by O4 to O7. The O–Dy distances fall into two regimes: 2.300(2)–2.332(2) Å and 2.423(2)/2.433(2) Å. The two longer distances are found for the amide oxygen (O7-Dy) and capping water (O3-Dy1). The Dy–N distances are in the range from 2.600(2) to 2.657(2) Å.

In the Dy-complex, a significant void with ill-defined solvent molecules was identified. The best solution was found with ten positions with high electron density in this void. However, the diffuse nature of these contributions prompted us to treat this cavity using the solvent masking algorithm implemented in OLEX2.[42] We identified a void centered on the crystallographic position −0.282 0.000 0.500 of approx. 693 Å^3 containing *ca.* 197 electrons. In the final solution after solvent masking, only the coordinated water (O3) has been refined.

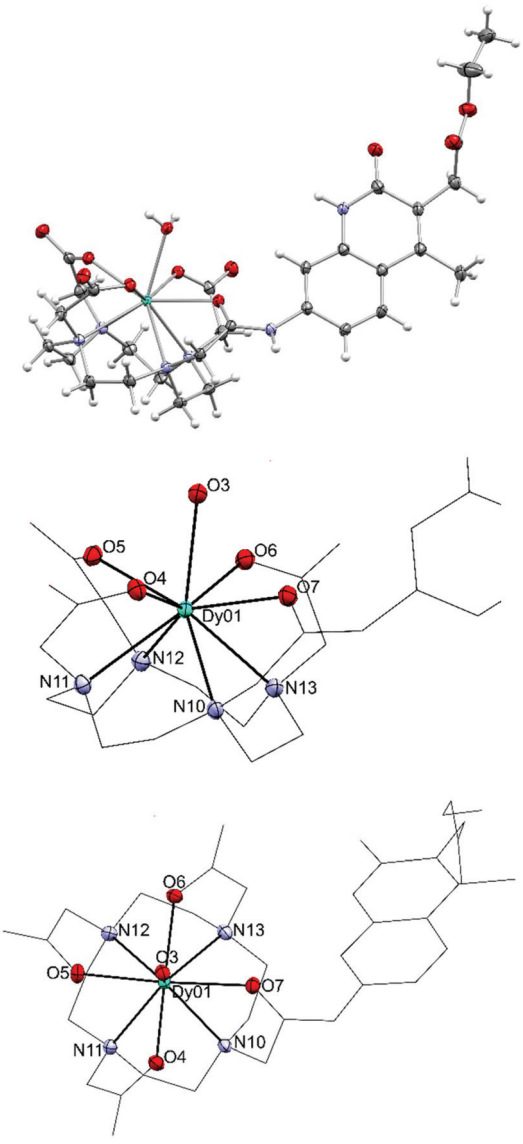

Fig. 3 Crystal structure of **Dy9d** (top), and side (middle) and top views (bottom) of the metal coordination sphere. Thermal ellipsoids are shown at the 50% probability levels.

Absorption and emission spectroscopy

The photophysical characterisation of **Ln1a–d** was done on [**Ln1a–d**] = 3 × 10^{-5} M solutions in 0.01 M aqueous PIPES buffer at pH 6.5. These conditions were chosen because previously we observed that Ln complexes with trifluoromethylated carbostyril antennae showed a reversible loss in Ln emission at pH > 7.[39] Analysis of the spectral shape of such Eu complexes showed no changes in the coordination environment, suggesting that deprotonation occurred in a non-coordinated group. As we could not exclude the loss of the core N–H proton, we have decided to do our experiments at a pH where deprotonation is not significant.

The absorption and emission data are summarised in Tables 1–4. All absorption and emission spectra are given in the ESI (Fig. S3–S13†). Compared to the non-*N*-alkylated **Ln9a–d**, the new complexes had slightly blue-shifted absorption and emission maxima (by 5–6 and 1–2 nm, respectively). The exception was the emission of **Ln1b**, which was red-shifted by 3 nm. In all cases, the change was small. The complexes had appreci-

Table 1 Antenna and Ln emissions in **Ln1a–d**, and comparisons with **Ln9a–d**[a]

Ligand	Ln	Φ_L[b]	Φ_{Ln}[b]
1a	Eu	1.5 (×3[c])	6.0 (×1.94[c])
	Tb	5.9 (×1.05[c])	**43.4** (×1.23[c])
	Gd	6.8 (**×0.88**[c])	—
1b	Eu	2.7 (×1.6[c])	**11.6** (×1.47[c])
	Tb	3.1 (×0.69[c])	15.9 (**×5.3**[c])
	Gd	3.2 (**×0.65**[c])	—
1c	Eu	2.5 (×6.25[c]) *2.6*[d]	8.9 (×1.89[c]) *9.2*[d]
	Tb	4.5 (×0.82[c]) *4.6*[d]	**45.1** (×1.96[c]) *47.9*[d]
	Gd	5.1 (**×0.74**[c])	—
1d	Eu	1.7 (×4.05[c]), *1.9*[d]	5.85 (×2.1[c]), *5.5*[d]
	Tb	7.1 (×1.11[c]), *7.0*[d]	**41.7** (×4.2[c]), *39.9*[d]
	Gd	7.7 (**×0.87**[c]), *7.7*[d]	—

[a] In pH 6.5 PIPES buffer, [**Ln1**] = 3 × 10^{-5} M; λ_{ex} = 336 (**Ln1a**), 348 (**Ln1b**), 338 (**Ln1c,d**) nm. [b] Using quinine sulfate as the reference. [c] Fold increase compared to **Ln9** reference compound, calculated from data from ref. 39. Unbuffered solutions, pH 6–7, see ref. 39. Quantum yields have an error of 10%. Values given in italics were recorded in a second set of independent measurements. [d] In water, measured under the same conditions as reported for **Tb9d**.

Table 2 Photophysical properties of the Gd complexes[a]

Complex	λ_{max}/nm	λ_{em}/nm	$E_{00}(S_1)$/cm^{-1}	$E_{00}(T_1)$/cm^{-1}	$\Delta(S_1–T_1)$/cm^{-1}
Gd1a	323 (−6)[b]	364 (−2)[b]	29 200 (+400)[b]	23 900 (+400)[b]	±0
Gd1b	337 (−5)[b]	393 (+3)[b]	27 550 (+50)[b]	23 100 (+700)[b]	−650
Gd1c	326 (−6)[b]	374 (−1)[b]	28 700 (+400)[b]	23 900 (+400)[b]	±0
Gd1d	326 (−5)[b]	368 (−2)[b]	28 900 (+300)[b]	23 400 (+400)[b]	−100

[a] In pH 6.5 PIPES buffer, [**Gd1**] = 3 × 10^{-5} M. [b] In parentheses: change from **Gd9a–d**, calculated from ref. 39.

Table 3 Radiative lifetimes, intrinsic quantum yields and sensitisation efficiencies of **Eu1a–d** and **Eu9a–d**[a]

Ligand	τ_{rad}/ms	τ_{obs}/ms	Φ_{Eu}^{Eu}	η_{sens}	Φ_{Eu}^{Eu} ratio[c]	Φ_{Eux}^{Eu} ratio[d]	η_{Eux} ratio[e]
1a	5.40	0.65	12.0	49.9	1.10	1.94	1.76
9a[b]	5.41	0.59	10.9	28.4			
1b	5.36	0.66	12.2	94.7	1.07	1.47	1.38
9b[b]	5.39	0.615	11.5	68.8			
1c	5.36	0.66	12.2	72.8	1.07	1.89	1.77
9c[b]	5.40	0.613	11.4	41.1			
1d	5.34	0.65	12.2	48.4	1.07	2.09	1.94
9d[b]	5.38	0.60	11.2	24.9			

[a] Calculated according to ref. 45. [b] Values taken from or calculated based on data reported in ref. 39. [c] Ratio of the intrinsic quantum yields of **Eu9x** and **Eu1x**. [d] Ratio of the overall quantum yields of **Eu9x** and **Eu1x**. [e] Ratio of the sensitisation efficiencies of **Eu9x** and **Eu1x**.

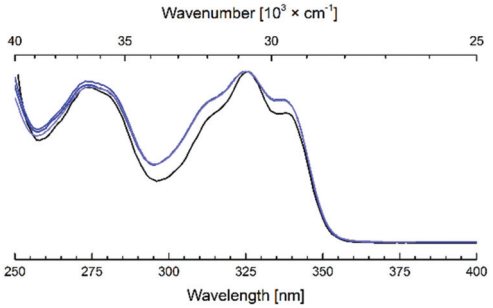

Fig. 4 Overlaid absorption (black) and excitation (blue) spectra of **Ln1d**, (Ln = Eu, Tb, Gd). For **Gd1d** the excitation spectrum corresponds to the antenna fluorescence (λ_{em} = 374 nm), for **Eu1d** and **Tb1d** excitations of the Ln-emissions are shown (λ_{em} = 700 and 545 nm, respectively), [**Ln1d**] = nominally 3.0 × 10^{-5} M, PIPES-buffered aqueous solutions 0.01 M, pH 6.5, Ln = Eu, Tb, Gd.

Table 4 Emission lifetimes and hydration numbers of **Ln1a–d**

Ligand	Ln[a]	τ_{H_2O}	τ_{D_2O}	q[b]
1a	Eu	0.65	2.18	1.0
	Tb	1.91	3.11	0.7
1b	Eu	0.66	2.16	1.0
	Tb	0.7	1.34	—
1c	Eu	0.66	2.17	1.0
	Tb	1.81	2.92	0.8
1d	Eu	0.65	2.16	1.0
	Tb	1.56	2.47	0.9

[a] λ_{ex} = 336 (**Ln1a**), 348 (**Ln1b**), 338 (**Ln1c,d**) nm; λ_{em} = 615 nm (Eu), 545 nm (Tb), initial delay: 0.05 ms; increments were adjusted between 0.2–10 μs depending on the lifetime. Lifetimes are reported as the average of three independent measurements. [b] Calculated as in ref. 17.

able absorptions at 337 nm, which is beneficial for laser-excitation without causing excessive damage to biomolecules.[2]

The carbostyril emissions (Φ_L) in **Gd1a–d** were weaker than in the non-alkylated complexes **Gd9a–d** (Table 1). While we did not have crystals of **Ln1**, in its precursor **5a**, which has a tertiary amide, the least squares planes (l.s.pl.) of the amide and the chromophore deviate by 86.72(14)°. This is reduced to 29.30(12)° in **Dy9d**, which has a secondary amide linker. Thus, there is essentially no orbital overlap between the tertiary amide and the heterocycle. In **Dy9d** (Fig. 3, synthesised previously, crystal structure not reported[39]) the amide and the heterocycle are more co-planar, which should be beneficial for the charge transfer excited state.[43] The more efficiently electron-donating substituent of **Ln9a–d** yields a more polar emitting state in **Ln9a–d** than in **Ln1a–d**. This is consistent with the slightly higher Φ_L in **Ln9a–d**, although the changes are small (Table 1).

All Eu and Tb complexes had robust Ln-centred emission upon antenna excitation. The **Ln1** absorption spectra and the Eu and Tb excitation spectra were similar, as expected for sensitised Ln emission (Fig. 4 and S3–S10†). Ln emissions were at 490, 545, 580, 620, 650, 667 and 680 nm for Tb and at 580, 590, 615, 655 and 700 nm for Eu, corresponding to the $^5D_4 \rightarrow {}^7F_J$ (J = 6–0) and $^5D_0 \rightarrow {}^7F_J$ (J = 0–6) transitions, respectively (Fig. 5). In all Eu complexes the major transition was the $^5D_0 \rightarrow {}^7F_4$ one, as in the **Ln9a–d** complexes. Every single one of the *N*-alkylated Eu and Tb complexes had higher Ln emission quantum yields than their non-alkylated analogues, **Ln9** (Table 1). **Tb1**, with the exception of **Tb1b**, had Φ_{Ln} > 40%. The best result was obtained for MOM-functionalised **Tb1c**, Φ_{Ln} = 45%. **Tb1c** had a fourfold higher Φ_{Ln} than **Tb9c**, while for **Tb1b** a 5.3-fold increase was noted (to 15.9%) from non-*N*-alkylated **Tb9b**. **Eu1** were less emissive than **Tb1**, with Φ_{Ln} in the 5.9–11.6% range; still, these values are in some cases twice as high as in the analogous **Eu9** complexes.

Antenna triplet states obtained from the phosphorescence bands at 77 K were located at 23 100–23 900 cm^{-1} in **Gd1** (Table 2). Trifluoromethylated **Gd1b** had the lowest-lying antenna triplet, at 23 100 cm^{-1}. The triplet states were 400–700 cm^{-1} higher in energy than in **Gd9a–d**. Tb and Eu have excited states at 20 400 (Tb), 19 000 ($^5D_1$, Eu) and 17 200 ($^5D_0$, Eu) cm^{-1}.[2,14] A general rule is that good triplet-mediated

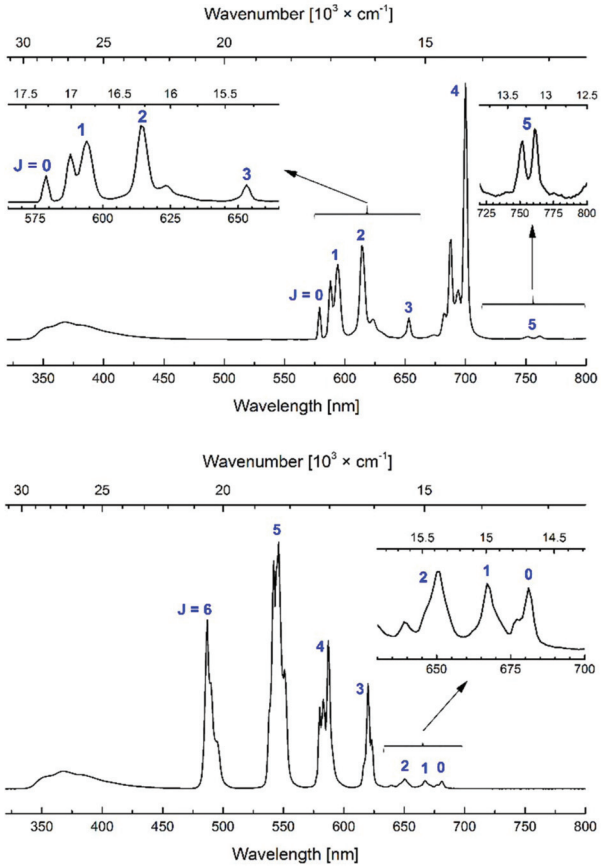

Fig. 5 Steady-state emission spectra of **Eu1d** (top) and **Tb1d** (bottom). [**Ln1d**] = nominally 3.0 × 10^{-5} M, PIPES-buffered aqueous solutions 0.01 M, pH 6.5; λ_{ex} = 336 nm.

sensitisation requires an antenna triplet-Ln excited state energy gap of 2500–3500 cm^{-1}.[13] Previous studies have shown that a minimal energy gap of 2000–2500 cm^{-1} is required to avoid energy back transfer; energy transfer is then improved with an increasing energy gap until ~24 000 cm^{-1} for Tb.[44] The presence of multiple acceptor levels in Eu makes the energy gap relation more complicated.[44] Thus, **1a–d** should be excellent sensitising ligands for both Eu and Tb, with the possible exception of **1b**, which may be too low-lying for Tb.

In the case of the Eu complexes the increased Φ_{Ln} appears to be in large part due to improved sensitisation efficiencies for all the antennae (Table 3). Quantum yield determinations carry ~10% relative error, and Φ_{Eu}^{Eu} should therefore be compared cautiously. Still, Φ_{Eu}^{Eu} of **Eu1a–d** are within experimental error (±0.1 ms) of those of **Eu9a–d**. This is expected based on the similarities of the coordination spheres (Fig. S11†). The observed lifetimes and the intrinsic quantum yields are identical within experimental error within the group of **Eu1a–d**. Interestingly, in a previous study, an Eu complex with the same Ln binding site and a tertiary amide-linked 7-amidocoumarin antenna had a very similar observed lifetime, 0.65 ms, while a non-alkylated analogue had τ_{obs} ~ 0.6 ms.[39] Thus, *N*-alkylation indeed increases the Eu lifetime and the intrinsic quantum yield, probably because of the removal of the N–H oscillator.

Most of the gain in overall quantum yield comes from the better sensitisation efficiency, η_{sens}. This is the product of the population of the feeding level (here, the antenna triplet), and the efficiency of the energy transfer. The triplet population is dependent on the efficiency of intersystem crossing, which will be affected by the S_1–T_1 energy gap, which was calculated in both **Gd1a–d** and **Gd9a–d** (Table 2). The differences are small, typically within experimental error, and are thus unlikely to have substantially benefited ISC; a possible exception is trifluoromethylated **Ln1b**. Energy transfer is dependent on the spectral overlap, on orientation factors, and on the donor–acceptor distance. In solution, the latter two are difficult to pin down, despite observations in the solid state. However, the small blue shifts of the **Gd1a–d** T_1 states compared to **Gd9a–d** may allow for a better spectral overlap.

The increased Ln emission is not caused by a decrease in the number of inner sphere solvent (water) molecules, which would increase the intrinsic quantum yield (Table 4). This is not surprising. The added carboxylate is not well disposed for Ln coordination, as that would form an unfavored 8-membered ring. The shape of the **Eu1** and **Eu9** emission spectra are very similar, as expected for complexes with similar metal coordination environments (Fig. S11†). The *q*-values determined for **Eu1** are the same as the values obtained for their **Eu9** analogues within experimental error (1.0 *vs.* 1.0–1.1).[39] For Tb complexes the *q*-values were lower than for the Eu species, which is consistent with Tb(III) being the smaller ion. The exception was **Tb1b**, for which an unrealistic result (q = 5) was obtained. As the antenna triplet in **Tb1b** is only 1800 cm^{-1} above the Tb excited state, this is likely due to energy back transfer. Substantial non-X–H-caused quenching makes the determination of q unreliable. In the case of back energy transfer the antenna triplet is repopulated, which in turn can be quenched by *e.g.* atmospheric oxygen.

The Ln complexes had modest antenna fluorescence emissions (Φ_L). In **Tb1a–d** Φ_L were 87–97% of those in **Gd1a–d** (Table 1), which may be due to ET from the carbostyril singlet excited state to the Tb. This has been seen before in both coumarin and carbostyril sensitised species.[39] Tb and Gd may also have different heavy atom effects, although these are usually assumed to be similar. PeT can be excluded for Tb and Gd complexes.

The drop in Φ_L was larger in **Eu1a–d** than in **Tb1a–d**. Antennae retained only 22–84% of the Φ_L of the appropriate **Gd1a–d** complexes. PeT and singlet ET could both contribute to this decrease. PeT from the excited carbostyril antennae to Eu^{3+} was found to be an efficient quenching pathway in **Eu9**.[39] The Φ_L decrease was smaller in **Eu1a–d** than in **Eu9a–d**, which may reflect decreased PeT due to the increased overall negative charge,[41] or less efficient singlet ET. However, it is important to emphasize that the observed changes in Φ_L in **Tb1a–d** and **Eu1a–d** compared to **Gd1a–d** do not support a substantial singlet mediated ET, and the contribution of the singlet state to Ln emission is small.

Experimental

Materials and methods

General procedures. ^{1}H NMR (400 MHz) and ^{13}C NMR (100 MHz) spectra were recorded on a JEOL 400 MHz instrument, respectively. Chemical shifts were referenced to residual solvent peaks and are given as follows: chemical shift (δ, ppm), multiplicity (s, singlet; br, broad; d, doublet, t, triplet; q, quartet; m, multiplet), coupling constant (Hz), integration. LC-MS analysis was carried out using Agilent 1100 and Waters micromass ZQ tandem system. HR-ESI-MS analyses were performed at the Organisch Chemisches Institut WWU Münster, Germany. All compounds displayed the expected isotope distribution pattern. Anhydrous CH_2Cl_2 was obtained by distillation from CaH_2 under an Ar atmosphere.

Compounds **1a**,[46] **1b**,[46] **1c**,[47] **1d**,[40] and **8c**,[39] were synthesised following literature methods. All other chemicals were from commercial sources and used as received.

Chromatography. Preparative chromatography was carried out on silica gel [Normasil 60 chromatographic silica media (40–63 micron)]. Thin layer chromatography was performed on silica-coated (60G F254) glass plates from Merck. Samples were visualised by UV-light (254 and 365 nm).

HPLC-analysis was performed on a RP-HPLC was performed on a Dionex UltiMate 3000 system using a Phenomenex Gemini® C18 TMS end-capped 150 mm × 4.6 mm HPLC column with water (0.05% formic acid) : CH_3CN (0.05% formic acid) eluent system using the methods: 0–10 min: 10% → 90% CH_3CN, 0–12 min: 10% → 50% CH_3CN, 0–8 min: 10 → 20% & 8–12 min: 20% iso CH_3CN. Flow rate: 0.5 mL min^{-1}, UV- (UltiMate 3000 Photodiode Array Detector) and ESI-MS detections (LCQ DECA XP MAX) were used.

Spectroscopy. All measurements were performed in PIPES buffered distilled water at pH 6.5. [Ln1] was nominally 3×10^{-5} M, however, small quantities of silica and Ln salts may diminish this. Glycerol was of 99.9+% purity. Quartz cells with 1 cm or 0.2 cm optical pathlengths were used for the room temperature measurements. The absorbance spectra were measured by a Varian Cary 100 Bio UV-Visible spectrophotometer. The emission and excitation spectra, lifetimes, time-resolved spectra and quantum yields were recorded on a Horiba FluoroMax-4P. All emissions were corrected by the wavelength sensitivity (correction function) of the spectrometer. All measurements were performed at room temperature unless stated otherwise.

Quantum yields were measured at room temperature and relative to quinine sulfate (QS) in H_2SO_4 0.05 M, $\Phi_{QS} = 0.59(1)$. Quantum yields were calculated according to (1), with Φ_s the quantum yield of the sample, Φ_{ref} the quantum yield of the reference, I the integrated corrected emission intensity of the sample (s) and of the reference (ref), f_A the absorption factor of the sample (s) and of the reference (ref) at the excitation wavelength and n the refractive indexes of the sample (s) and of the reference (ref). The concentration of the complexes was adjusted to obtain an absorbance around the maxima of the antennae matching that of the QS fluorescent standard. The excitation wavelength where the absorption factors of the samples and of the reference were the same was chosen (*i.e.* where the absorptions are identical). The corrected emission spectra of the sample and reference standard were then measured under the same conditions over the 330–800 nm spectral range as well as blank samples containing only the solvent (*i.e.* water or PIPES buffered aqueous solutions). The appropriate blanks were subtracted from their respective spectra, and the antenna fluorescence and lanthanide luminescence were separated by fitting the section of the antenna emission overlapping the lanthanide emission with an exponential decay or with a scaled emission spectrum from the corresponding gadolinium complexes. The quantum yields were then calculated according to (1). The given relative error on the quantum yields ($\delta\Phi = \Delta\Phi/\Phi$, where $\Delta\Phi$ is the absolute error) take into account the accuracy of the spectrometer and of the integration procedure [$\delta(I_s/I_{ref}) < 2\%$], an error of 0.59 ± 0.01 on the quantum yield of the reference QS [$\delta(\Phi_{ref}) < 2\%$], an error on the ratio of the absorption factors [$\delta(f_{Aref}/f_{As}) < 5\%$, relative to the fixed absorption factor of the reference QS] and an error on the ratio of the squared refractive indexes [$\delta(n_s^2/n_{ref}^2) < 1\%$, <0.25% around 1.333 on each individual refractive index], which sums to a total estimated relative error that should be $\delta\Phi_s < 10\%$. A limit value of 10% is thus chosen.

$$\Phi = \frac{I_s}{I_{ref}} \cdot \frac{f_{Aref}}{f_{As}} \cdot \frac{(n_s)^2}{(n_{ref})^2} \cdot \Phi_{ref} \quad (1)$$

Low temperature measurements were done in quartz capillaries at 77 K by immersion in a liquid N_2-filled quartz Dewar and with addition of glycerol (1 drop) to the solutions (9 drops) measured at room temperature.

Lifetimes were recorded 0.05 ms after pulsed excitations at the excitation maxima (λ_{ex}) between 300–400 nm by measuring the decay of the lanthanide main emission peak (*i.e.* Eu 615 nm, Tb 545 nm). The increments after the initial delay were adjusted between 0.2–10 μs depending on the lifetime in order to have a good sampling of the decay. The obtained data were fitted by mono and double exponential decay models in OriginPro 9, and the most reliable value was chosen according to the adjusted R^2 value and the shape of the residuals. A relative error of 10% is typically found among a series of measurements on the same sample.

Hydration numbers q were obtained by measuring the lifetimes of the same quantity of complex in an unbuffered solution in H_2O and in D_2O and fitting the difference according to the model of Horrocks *et al.*,[16] and Beeby *et al.*[17]

X-ray diffraction data. Measurements were performed using graphite-monochromatised Mo K_α radiation at 150 K using a Bruker D8 APEX-II equipped with a CCD camera. The structure was solved by direct methods (SHELXS-2014) and refined by full-matrix least-squares techniques against F^2 (SHELXL-2018).[48] The non-hydrogen atoms were refined with anisotropic displacement parameters. The H atoms of the CH_2/CH groups were refined with common isotropic displacement parameters for the H atoms of the same group and ideal-

ised geometry. The H atoms of the methyl groups were refined with common isotropic displacement parameters for the H atoms of the same group and idealised staggered geometry; one methyl group is modelled as a disordered staggered configuration.

*Specific for **5a**.* NH protons are located on the difference map or placed at idealised positions. The cyclen ring shows a positional disorder which is modelled with an occupancy of 0.53 and 0.47 of the two different orientations, respectively.

*Specific for **Dy9d**.* Solvent accessible voids were treated using the solvent masking algorithm implemented in OLEX2 accounting for a 197 electrons in a 693 Å^3 large void. In addition a structure refinement prior to applying solvent masking is attached.

CCDC 1832851 and 1833918 contain the supplementary crystallographic data for this paper.

Synthetic procedures

General procedure for synthesis of compounds 3a–d. The appropriate carbostyril (**2a–d**) was dissolved in DMF (250 mM). DIPEA (3.0 equiv.), and then the alkylating agent (*tert*-butyl bromoacetate, 1.2 equiv.) were added. The reaction mixture was stirred at room temperature, and the progress of the reaction was monitored by TLC analysis. A further 2.4 equiv. of alkylating agent was added in each case to drive the reaction to completion. When necessary, more base was also added. Once TLC analysis indicated the completion of the reaction, the mixture was poured into a separation funnel, and CH_2Cl_2 and H_2O were added. The phases were separated, and the aqueous phase was extracted again with CH_2Cl_2. The combined organic phases dried over $MgSO_4$, filtered, and the filtrate was concentrated under reduced pressure. Residual DMF was co-evaporated with toluene. The crude products were purified by column chromatography on silica gel using the following eluent mixtures: CH_2Cl_2 : AcOEt : ^{i}PrOH (6 : 4 : 0 → 6 : 3 : 1) for **3a**, CH_2Cl_2 : Et_2O : acetone (8 : 2 : 0 → 7 : 3 : 0 → 7 : 1.5 : 1.5) for **3b**, CH_2Cl_2 : Et_2O (3 : 2 iso) for **3c**, CH_2Cl_2 : Et_2O : acetone (8 : 2 : 0 → 5 : 5 : 0 → 5 : 3 : 2) for **3d**.

3a. 1.057 g (61% → 41% after recrystallization +20% after col. chrom. on the filtrate); ^{1}H NMR (400 MHz, DMSO-d_6) δ ppm 1.43 (3, 9H), 2.29 (s, 3H), 3.79 (d, J = 6.3 Hz, 2H), 5.99 (s, 1H), 6.25 (d, J = 2.1 Hz, 1H), 6.52 (dd, J = 8.8 Hz, 2.2 Hz, 1H), 6.64 (t, J = 6.1 Hz, 1H), 7.39 (d, J = 8.8 Hz, 1H), 11.22 (s, 1H); ^{13}C NMR (101 MHz, DMSO-d_6) δ ppm 18.4 (CH_3), 27.7 (CH_3), 45.0 (CH_2), 80.8 (C_q), 94.8, 109.4, 110.8, 115.2, 125.4, 140.7, 147.9, 162.3, 169.9; RP-HPLC t_R = 6.13 min (10 min method 10% → 90%); ESI-MS obsd 289.02; HR-ESI-MS obsd 311.1373, calcd 311.1366 [(M + Na)$^+$, M = $C_{16}H_{20}N_2O_3$].

3b. 1.302 g, (43% → 34% after recrystallization +9% after col. chrom. on the filtrate); ^{1}H NMR (400 MHz, DMSO-d_6) δ ppm 1.43 (s, 9H), 3.83 (d, J = 4.7 Hz, 2H), 6.34 (d, J = 1.9 Hz, 1H), 6.49 (s, 1H), 6.65 (dd, J = 9.0, 2.2 Hz, 1H), 7.04 (brd, 1H), 11.92 (s, 1H); ^{13}C NMR (101 MHz, DMSO-d_6) δ ppm 27.7 (CH_3), 44.8 (CH_2), 81.0 (C_q), 94.8 (CH_{Ar}), 104.0 (CH_{Ar}), 111.1 (CH_{Ar}), 114.2 (CH), 122.9 (C_q), 124.2 (C_{Ar}), 136.7 (C_q) 142.1 (C_{Ar}), 151.0 (C_{Ar}), 160.8 (C_q), 169.5 (C_q); ^{19}F NMR (376 MHz, DMSO-d_6) δ ppm −62.3; RP-HPLC t_R = 6.97 min (10 min method 10% → 90%); ESI-MS obsd 342.99; HR-ESI-MS obsd 365.1075, calcd 365.1083 [(M + Na)$^+$, M = $C_{16}H_{17}NF_3N_2O_3$].

3c. 1.954 g (84% → 49% after recrystallization +35% after col. chrom. on the filtrate); ^{1}H NMR (400 MHz, DMSO-d_6) δ ppm 1.42 (s, 9H), 3.36 (s, 3H), 3.79 (d, J = 6.4, 2H), 4.54 (s, 2H), 6.13 (s, 1H), 6.27 (d, J = 2.2 Hz, 1H), 6.51 (dd, J = 8.8, 2.2 Hz, 1H), 6.67 (t, J = 6.4 Hz, 1H), 7.37 (d, J = 8.8 Hz, 1H), 11.35 (s, 1H); ^{13}C NMR (101 MHz, DMSOd$_6$) δ ppm 28.2 (CH_3), 45.0 (CH_2), 58.0 (CH_3), 70.5 (CH_2), 80.8 (C_q), 94.8 (CH_{Ar}), 108.4 (CH_{Ar}), 109.6 (CH_{Ar}), 113.3 (CH), 124.9 (CH_{Ar}), 141.0 (C_q), 147.3 (C_{Ar}), 150.2 (C_{Ar}), 162.4 (C_q), 169.9 (C_q); RP-HPLC t_R = 6.03 min (10 min method 10% → 90%); ESI-MS obsd 318.65; HR-ESI-MS obsd 341.1469, calcd 341.1472 [(M + Na)$^+$, M = $C_{17}H_{22}N_2O_4$].

3d. 3.72 g (76%); ^{1}H NMR (400 MHz, $CDCl_3$) δ ppm 1.25 (t, J = 7.1 Hz, 3H), 1.51 (s, 9H), 2.43 (s, 3H), 3.80 (s, 2H), 3.88 (s, 2H), 4.17 (q, J = 7.1 Hz, 2H), 6.38 (d, J = 2.3 Hz, 1H), 6.62 (d, J = 8.9, 2.3 Hz, 1H), 7.54 (d, J = 8.9 Hz, 1H), 11.59 (s, 1H); ^{13}C NMR (101 MHz, $CDCl_3$) δ ppm 14.3 (CH_3), 15.5 (CH_3), 28.2 (CH_3), 32.5 (CH_2), 46.0 (CH_2), 60.8 (CH_2) 82.4 (C_q), 96.6 (CH_{Ar}), 110.3 (C_{Ar}), 112.9 (CH_{Ar}), 119.2 (C_q), 125.9 (CH_{Ar}), 139.3 (C_q), 146.1 (C_{Ar}), 148.8 (C_{Ar}), 163.7 (C_q), 170.0 (C_q), 171.8 (C_q); RP-HPLC t_R = 6.73 min (10 min method 10% → 90%); ESI-MS obsd 374.71; HR-ESI-MS obsd 397.1730, calcd 397.1724 [(M + Na)$^+$, M = $C_{20}H_{26}N_2O_5$].

General procedure for synthesis of compound 4a–d. Samples of **3a–d** were dissolved in 1 : 1 mixture of DMF and distilled CH_2Cl_2 (125 mM). The solutions were cooled to 0 °C and 2,6-di-*tert*-butyl-pyridine (3.0 equiv.) was added followed by the addition of chloroacetyl chloride (1.2 equiv.). The reaction mixtures were then allowed to warm to room temperature. When TLC analysis indicated the completion of the reaction, the mixture was diluted with H_2O and EtOAc. The phases were separated, and the aqueous layer was extracted with EtOAc. The combined organic phases were dried over $MgSO_4$, filtered, and the filtrate was concentrated at reduced pressure. The crude products were purified by column chromatography on silica gel using the following eluent mixtures: CH_2Cl_2 : Et_2O : ^{i}PrOH (8 : 2 : 0 → 8 : 1 : 1) for **4a**, $CHCl_3$: Et_2O : EtOH (9.5 : 0.5 : 0 → 8 : 2 : 0 → 8 : 1.6 : 0.4) for **4b**, $CHCl_3$: Et_2O : ^{i}PrOH (9 : 1 : 0 → 8.5 : 1.5 : 0 → 8.5 : 1 : 0.5) for **4c**, CH_2Cl_2 : Et_2O : EtOH (9.5 : 0.5 : 0 → 8 : 2 : 0 → 8 : 1.6 : 0.4) for **4d**.

4a. 0.818 g (83%); ^{1}H NMR (400 MHz, DMSO-d_6) δ ppm 1.42 (s, 9H), 2.43 (s, 3H), 4.13 (s, 2H), 4.29 (s, 2H), 6.44 (s, 1H), 7.23 (d, J = 8.0 Hz, 1H), 7.32 (s, 1H), 7.79 (d, J = 8.5 Hz, 1H), 11.75 (s, 1H); ^{13}C NMR (101 MHz, DMSO-d_6) δ ppm 18.5 (CH_3), 27.7 (CH_3), 41.8 (CH_2), 52.4 (CH_2), 81.5 (C_q), 114.1 (C_q), 119.4 (C_{Ar}), 120.9 (CH_{Ar}), 121.5 (CH), 126.3 (CH_{Ar}), 139.4 (C_q), 142.8 (C_{Ar}), 147.5 (C_{Ar}), 161.7 (C_q), 165.7 (C_q), 167.6 (C_q); RP-HPLC t_R = 6.23 min (10 min method 10% → 90%); ESI-MS obsd 364.97; HR-ESI-MS obsd 387.1081, calcd 387.1082 [(M + Na)$^+$, M = $C_{18}H_{21}ClN_2O_4$].

4b. 1.80 g (quant.); ^{1}H NMR (400 MHz, DMSO-d_6) δ ppm 1.42 (s, 9H), 4.19 (s, 2H), 4.32 (s, 2H), 7.03 (s, 1H), 7.35 (s, J = 8.5 Hz, 1H), 7.46 (s, 1H), 7.77 (d, J = 8.5 Hz, 1H), 12.48 (s, 1H);

^{13}C NMR (101 MHz, DMSO-d_6) δ ppm 27.7 (CH_3), 41.9 (CH_2), 52.2 (CH_2), 81.6 (C_q), 112.6 (C_{Ar}), 115.0 (CH_{Ar}), 121.0 (CH_{Ar}), 122.3 (CH), 122.4 (q, J = 275 Hz, C_q), 125.7 (CH_{Ar}), 136.2 (q, J = 32.2 Hz, C_q), 140.6 (C_{Ar}), 144.0 (C_{Ar}), 160.2 (C_q), 165.7 (C_q), 167.6 (C_q); ^{19}F NMR (376 MHz, DMSO-d_6) δ ppm −62.5; RP-HPLC t_R = 7.03 min (10 min method 10% → 90%); ESI-MS obsd 419.94; HR-ESI-MS obsd 441.0795, calcd 441.0799 [$(M + Na)^+$, M = $C_{18}H_{18}ClF_3N_2O_4$].

4c. 1.78 g (87% → 68% after recrystallization (from EtOAc twice before chromatography) + 19% after col. chrom. on the filtrate); ^{1}H NMR (400 MHz, DMSO-d_6) δ ppm 1.42 (s, 9H), 3.39 (s, 3H), 4.14 (s, 2H), 4.29 (s, 2H), 4.66 (s, 2H), 6.53 (s, 1H), 7.22 (d, J = 8.0 Hz, 1H), 7.35 (s, 1H), 7.75 (d, J = 8.6 Hz, 1H), 11.88 (s, 1H); ^{13}C NMR (101 MHz, DMSO-d_6) δ ppm 27.7 (CH_3), 40.2 (CH_2), 52.3 (CH_2), 58.6 (CH_3), 70.2 (CH_2), 81.5 (C_q), 114.3 (CH_{Ar}), 117.2 (C_{Ar}), 119.9 (CH_{Ar}), 120.9 (CH), 125.8 (CH_{Ar}), 139.7 (C_q), 142.9 (C_{Ar}), 146.8 (C_{Ar}), 161.6 (C_q), 165.7 (C_q), 167.6 (C_q); RP-HPLC t_R = 6.20 min (10 min method 10% → 90%); ESI-MS obsd 394.97; HR-ESI-MS obsd 417.1183, calcd 417.1188 [$(M + Na)^+$, M = $C_{19}H_{23}ClN_2O_5$].

4d. 2.59 g (72%) (recrystallised from EtOAc after col. chrom.); ^{1}H NMR (400 MHz, DMSO-d_6) δ ppm 1.18 (t, J = 7.1 Hz, 3H), 1.42 (s, 9H), 2.40 (s, 3H), 3.72 (s, 2H), 4.07 (q, J = 7.1 Hz, 2H), 4.14 (s, 2H), 4.30 (s, 2H), 7.25 (d, J = 8.1 Hz, 1H), 7.33 (s, 1H), 7.86 (d, J = 8.6 Hz, 1H), 11.92 (s, 1H); ^{13}C NMR (101 MHz, DMSO-d_6) δ ppm 14.1 (CH_3), 15.3 (CH_3), 27.7 (CH_3), 32.2 (CH_2), 40.2 (CH_2), 52.4 (CH_2), 60.2 (CH_2), 81.4 (C_q), 113.9 (C_{Ar}), 119.5 (CH_{Ar}), 121.0 (C_q), 125.4 (CH_{Ar}), 126.6 (CH_{Ar}), 138.1 (C_q), 142.4 (C_{Ar}), 144.1 (C_{Ar}), 161.4 (C_q), 165.7 (C_q), 167.6 (C_q), 170.4 (C_q); RP-HPLC t_R = 6.83 min (10 min method 10% → 90%); ESI-MS obsd 451.03; HR-ESI-MS obsd 473.1446, calcd 473.1450 [$(M + Na)^+$, M = $C_{22}H_{27}ClN_2O_6$].

General procedure for synthesis of compound 5a–d. Cyclen was dissolved in $CHCl_3$ (633 mM). The vigorously stirred solution was treated with a solution of **4a–d** in $CHCl_3$: DMF (3 : 1) (158 mM). The reaction mixture was stirred for 1–2 days, when TLC analysis showed full conversion of the limiting starting material. The $CHCl_3$ was evaporated under reduced pressure, and the residue was diluted with a 1 : 1 mixture of CH_2Cl_2 and MeOH (few mL). This solution was loaded onto a silica column that had been conditioned with CH_2Cl_2 : MeOH (1 : 1). Elution with CH_2Cl_2 : MeOH : NH_4OH (10 : 9 : 1) yielded the products as white (**5a**), off-white (**5c**), yellowish-white (**5b**, **5d**) solids.

5a. 0.627 g (91%); ^{1}H NMR (400 MHz, DMSO-d_6) δ ppm 1.41 (s, 9H), 2.10–3.75 (m, 24H (21H product, 3.36H DMSO/H_2O/EtOH)), 4.22 (s, 2H), 6.40 (s, 1H), 7.17 (d, J = 7.9 Hz, 1H), 7.31 (s, 1H), 7.75 (d, J = 8.5 Hz, 1H); ^{13}C NMR (101 MHz, DMSO-d_6) δ ppm 18.5 (CH_3), 27.7 (CH_3), 44.9 (CH_2), 45.5 (CH_2), 46.6 (CH_2), 51.1 (CH_2), 52.0 (CH_2), 55.3 (CH_2) 81.2 (C_q), 113.8 (CH_{Ar}), 118.9 (C_{Ar}), 120.7 (CH_{Ar}), 121.2 (CH), 126.2 (CH_{Ar}), 139.4 (C_q), 143.5 (C_{Ar}), 147.6 (C_{Ar}), 161.8 (C_q), 168.0 (C_q), 170.0 (C_q); RP-HPLC t_R = 1.71, 4.05 min (16 min method: 0–12 min 10% → 50%); ESI-MS obsd 501.23; HR-ESI-MS obsd 501.3181, calcd 501.3184 [$(M + H)^+$, M = $C_{26}H_{40}N_6O_4$].

5b. 1.822 g (94%); ^{1}H NMR (400 MHz, DMSO-d_6) δ ppm 1.34–1.48 (s, 9H), 2.18–2.86 (m, 17.17H (16H product, 1.17H DMSO)), 3.29 (s, 2H), 4.25 (s, 2H), 4.99 (br., 3H), 6.93 (s, 1H), 7.21 (dd, J = 8.7, 1.2 Hz, 1H), 7.46 (d, J = 1.2 Hz, 1H), 7.70 (d, J = 7.3 Hz, 1H); ^{13}C NMR (101 MHz, DMSO-d_6) δ ppm 27.7 (CH_3), 45.0 (CH_2), 45.4 (CH_2), 46.7 (CH_2), 51.2 (CH_2), 51.9 (CH_2), 55.6 (CH_2), 81.2 (C_q), 112.3 (C_{Ar}), 116.1 (CH_{Ar}), 121.0 (CH_{Ar}), 121.5 (CH), 122.7 (q, J = 275.0 Hz, C_q), 125.3 (CH_{Ar}), 135.4 (q, J = 31.0 Hz, C_q), 142.7 (C_{Ar}), 144.2 (C_{Ar}), 161.7 (C_q), 168.0 (C_q), 170.2 (C_q); ^{19}F NMR (376 MHz, DMSO-d_6) δ ppm −62.3 RP-HPLC t_R = 5.37 min (16 min method: 0–12 min 10% → 50%); ESI-MS obsd 555.19; HR-ESI-MS obsd 555.2919, calcd 555.2901 [$(M + H)^+$, M = $C_{26}H_{37}F_3N_6O_4$].

5c. 1.681 g (81%); ^{1}H NMR (400 MHz, DMSO-d_6) δ ppm 1.34–1.50 (s, 9H), 2.11–2.99 (m, 17.76H (16H product, 1.76H DMSO/DMF)), 3.25 (br, 2H), 3.39 (s, 3H), 4.22 (s, 2H), 4.66 (s, 2H), 6.50 (s, 1H), 7.16 (d, J = 7.5 Hz, 1H), 7.35 (s, 1H), 7.71 (d, J = 8.5 Hz, 1H); ^{13}C NMR (101 MHz, DMSO-d_6) δ ppm 27.6 (CH_3), 44.9 (CH_2), 45.5 (CH_2), 46.6 (CH_2), 51.1 (CH_2), 51.9 (CH_2), 55.3 (CH_2), 58.2 (CH_3), 70.2 (CH_2), 81.2 (C_q), 114.0 (CH_{Ar}), 116.8 (C_{Ar}), 119.5 (CH_{Ar}), 120.7 (CH), 125.7 (CH_{Ar}), 139.7 (C_q), 143.6 (C_{Ar}), 146.8 (C_{Ar}), 161.7 (C_q), 168.0 (C_q), 170.0 (C_q); RP-HPLC t_R = 1.75, 2.08, 4.12 min; (16 min method: 0–12 min 10% → 50%); ESI-MS obsd 531.24; HR-ESI-MS obsd 531.3292 calcd 531.3289 [$(M + H)^+$, M = $C_{27}H_{42}N_6O_5$].

5d. 2.84 g (89%); ^{1}H NMR (400 MHz, DMSO-d_6) δ ppm 1.18 (t, J = 7.1 Hz, 3H), 1.42 (s, 9H), 2.19–2.93 (m, 22H (19H product, 3H DMSO)), 3.24 (s, 2H), 3.72 (s, 2H), 4.06 (q, J = 7.1 Hz, 2H), 4.23 (s, 2H), 7.19 (d, J = 7.8 Hz, 1H), 7.31 (s, 1H), 7.83 (d, J = 8.6 Hz, 1H); ^{13}C NMR (101 MHz, DMSO-d_6) δ ppm 14.1 (CH_3), 15.3 (CH_3), 27.7 (CH_3), 32.2 (CH_2), 45.0 (CH_2), 45.5 (CH_2), 46.7 (CH_2), 51.2 (CH_2), 52.0 (CH_2), 60.2 (CH_2), 81.2 (C_q), 113.6 (CH_{Ar}), 119.1 (C_{Ar}), 120.8 (CH_{Ar}), 125.0 (C_q), 126.5 (CH_{Ar}), 138.1 (C_{Ar}), 143.1 (C_{Ar}), 161.4 (C_q), 168.0 (C_q), 170.0 (C_q), 170.5 (C_q); RP-HPLC t_R = 1.88, 4.63, 5.50 min (16 min method: 0–12 min 10% → 50%); ESI-MS obsd 587.27; HR-ESI-MS obsd 587.3561, calcd 587.3552 [$(M + H)^+$, M = $C_{30}H_{46}N_6O_6$].

General procedure for synthesis of compound 6a–d. The appropriate monoalkylated cyclen (**5a–d**) were dissolved in DMF (60 mM). DIPEA (5.0 equiv.) was added to the solutions, followed by *tert*-butyl bromoacetate (3.0 equiv.). The reaction mixture was stirred at room temperature overnight. At this point HPLC analysis of the reaction mixture showed mostly full conversion, along with small quantities of dialkylated by-product. The mixture was concentrated under reduced pressure. Approximately 2/3 of the residual DMF was removed by co-evaporation with toluene (note: do not dry the mixture completely! If that happens the cyclen ring gets protonated by DIPEA·HBr making purification by column chromatography impossible). The crude product was purified by silica column chromatography by elution with $CHCl_3$ containing acetone with increasing quantities of MeOH (9 : 1 : 0 → 8 : 2 : 0 → 8 : 1 : 1). For analytically pure products, up to 3 columns were needed.

6a. 0.429 g (81%); ^{1}H NMR (400 MHz, $CDCl_3$) δ ppm 1.12–1.77 (m, 67H (36H product, 31H DIPEA·HBr)), 1.79–3.86 (m, 35.5 (27H product, 8.3H DIPEA·HBr, 0.2 solvent residues)), 4.05–4.40 (br, 2H), 6.46 (s, 1H), 7.09 (dd, J = 8.5 Hz, 1.9 Hz,

1H), 7.49 (d, J = 1.6 Hz, 1H), 7.65 (d, J = 8.6 Hz), 12.43 (s, 1H); ^{13}C NMR (101 MHz, $CDCl_3$) δ ppm 19.3 (CH_3), 27.9 (CH_3), 28.0 (CH_3), 48.0–49.0 (CH_2), 51.8–53.0 (CH_2), 52.8 (CH_2), 55.6 (CH_2), 55.7 (CH_2), 56.0 (CH_2), 81.9 (C_q), 82.0 (C_q), 114.9 (CH_{Ar}), 120.3 (C_{Ar}), 121.4 (CH), 121.4 (CH_{Ar}), 126.3 (CH_{Ar}), 139.5 (C_q), 143.0 (C_{Ar}), 148.4 (C_{Ar}), 163.8 (C_q), 167.4 (C_q), 171.6 (C_q), 172.6 (C_q); RP-HPLC t_R = 4.80 min (10 min method 10% → 90%); ESI-MS obsd 843.40; HR-ESI-MS obsd 865.5041, calcd 865.5046 [$(M + Na)^+$, M = $C_{44}H_{70}N_6O_{10}$].

6b. 0.759 g (66%); ^{1}H NMR (400 MHz, $CDCl_3$) δ ppm 1.14–1.74 (m, 45.9H (36H product, 9.9H DIPEA·HBr)), 1.77–3.90 (m, 30.66H (24H product, 0.96H DMF, 2.64H DIPEA·HBr)), 4.12–4.40 (br, 2H), 6.95 (s, 1H), 7.13 (dd, J = 8.7 Hz, 1.6 Hz, 1H), 7.68 (d, J = 8.0 Hz, 1H), 8.14 (d, J = 1.4 Hz, 1H), 12.64 (s, 1H); ^{13}C NMR (101 MHz, $CDCl_3$) δ ppm 27.9 (CH_3), 28.1 (CH_3), 48.0–49.3 (CH_2), 51.5–53.0 (CH_2), 52.1 (CH_2), 55.7 (CH_2), 55.8 (CH_2), 56.1 (CH_2), 81.7 (C_q), 81.9 (C_q), 113.8 (C_{Ar}), 116.2 (CH_{Ar}), 121.7 (CH_{Ar}), 122.4 (CH), 122.5 (q, J = 275 Hz, C_q), 125.9 (CH_{Ar}), 137.4 (q, J = 31.7 Hz, C_q), 141.2 (C_{Ar}), 143.6 (C_{Ar}), 161.0 (C_q), 167.5 (C_q), 171.6 (C_q), 172.7 (C_q); ^{19}F NMR (376 MHz, $CDCl_3$) δ ppm −63.5 RP-HPLC t_R = 4.97 min (10 min method 10% → 90%); ESI-MS obsd 897.36; HR-ESI-MS obsd 919.4767, calcd 919.4763 [$(M + Na)^+$, M = $C_{44}H_{67}N_6O_{10}F_3$].

6c. 0.505 g (53%); ^{1}H NMR (400 MHz, $CDCl_3$) δ ppm 1.30–1.74 (m, 41H (36H product, 5H DIPEA·HBr)), 1.78–4.49 (m, 32H (29H product, 1.33 H DIPEA·HBr, 1.67 H solvent residues)), 4.66 (s, 2H), 6.71 (s, 1H), 7.09 (dd, J = 8.6 Hz, 1.7 Hz, 1H), 7.50 (m, 1H), 7.67 (d, J = 8.6 Hz, 1H), 12.74 (s, 1H); ^{13}C NMR (101 MHz, $CDCl_3$) δ ppm 27.9 (CH_3), 28.1 (CH_3), 48.0–49.3 (CH_2), 52.0–53.5 (CH_2), 71.3 (CH_2), 81.8 (C_q), 82.0 (C_q), 115.1 (CH_{Ar}), 118.2 (C_{Ar}), 120.2 (CH_{Ar}), 121.6 (CH), 125.8 (CH_{Ar}), 139.9 (C_q), 147.5 (C_{Ar}), 164.0 (C_q), 167.5 (C_q), 171.7 (C_q), 172.7 (C_q); RP-HPLC t_R = 10.07 min (16 min method: 0–12 min 10% → 50%); ESI-MS obsd 873.37; HR-ESI-MS obsd 895.5151, calcd 895.5151 [$(M + Na)^+$, M = $C_{45}H_{72}N_6O_{11}$].

6d. 1.35 g (34%; yield of the analytically pure compound after the first column. A significant amount of **6d** was washed away by the residual DMF and came off with the front. This part of the batch was kept in storage. From this sample crystals grew that were suitable for X-ray analysis, and has thus not been worked up); ^{1}H NMR (400 MHz, $CDCl_3$) δ ppm 1.20 (t, J = 7.2 Hz, 3H), 1.24–1.73 (m, 36H), 1.82–3.74 (m, 27H), 3.81 (s, 2H), 4.10 (q, J = 7.1 Hz, 2H), 4.15–4.35 (br, 2H), 7.11 (dd, J = 8.6 Hz, 1.8 Hz, 1H), 7.45 (d, J = 1.6 Hz, 1H), 7.70 (d, J = 8.6 Hz, 1H), 11.90 (s, 1H); ^{13}C NMR(101 MHz, $CDCl_3$) δ ppm 14.3 (CH_3), 15.9 (CH_3), 27.9 (CH_3), 28.0 (CH_3), 28.1 (CH_3), 32.5 (CH_2), 48.0–49.0 (CH_2), 51.5–53.0 (CH_2), 55.7 (CH_2), 55.8 (CH_2), 56.0 (CH_2), 60.9 (CH_2), 81.8 (C_q), 114.9 (C_{Ar}), 120.6 (C_{Ar}), 121.8 (CH_{Ar}), 125.4 (C_q), 126.5 (CH_{Ar}), 138.4 (C_{Ar}), 142.5 (C_{Ar}), 145.2 (C_q), 162.9 (C_q), 167.4 (C_q), 170.8 (C_q), 171.7 (C_q), 172.3 (C_q); RP-HPLC t_R = 4.93 min (10 min method 10% → 90%) ESI-MS obsd 929.47; HR-ESI-MS obsd 951.5411, calcd 951.5413 [$(M + Na)^+$, M = $C_{48}H_{76}N_6O_{12}$].

General procedure for synthesis of compound 7a–d. The protected ligands **7a–d** were dissolved in CH_2Cl_2, and an equal volume of TFA was added (45 mM). The mixture was stirred overnight at room temperature. Full conversion was observed the following day by TLC analysis. The volatile components were evaporated under reduced pressure, and the TFA-residues were removed by repeated co-evaporation with toluene. The resulting viscous orange residue was dissolved in acetonitrile containing a small amount of water, and the solution was loaded onto a silica gel column that had been conditioned with acetonitrile : H_2O (9 : 1). Elution with acetonitrile : H_2O (9 : 1 → 7 : 3) yielded the ligands as white (**6a,c**) and yellowish-white (**6b,d**) solids.

7a. 208 mg (81%); ^{1}H NMR (400 MHz, D_2O) δ ppm 1.25–1.35 (m, 1.02H DIPEA), 1.84–4.65 (m, 29.3H (29H product, 0.3H DIPEA)), 6.31 (s, 1H), 7.27 (d, J = 8.4 Hz, 1H), 7.37 (s, 1H), 7.71 (d, J = 8.4 Hz, 1H); ^{13}C NMR (101 MHz, D_2O) δ ppm 16.3 (CH_3), 47.5–48.7 (CH_2), 52.2–53.2 (CH_2), 54.1 (CH_2), 56.5 (CH_2), 58.7 (CH_2), 58.9 (CH_2), 114.3 (CH_{Ar}), 119.4 (C_{Ar}), 120.3 (CH_{Ar}), 121.8 (CH), 126.8 (CH_{Ar}), 137.7 (C_q), 143.0 (C_{Ar}), 151.0 (C_{Ar}), 164.0 (C_q), 174.0 (C_q), 174.7 (C_q), 180.2 (C_q); RP-HPLC t_R = 3.02–7.12 min (16 min method: 0–12 min 10% → 50%); ESI-MS obsd 619.27; HR-ESI-MS obsd 655.2068, calcd 655.2046 [(M + Ca − 3H), M = $C_{28}H_{38}N_6O_{10}$].

7b. 434 mg (92%); ^{1}H NMR (400 MHz, D_2O) δ ppm 1.85–4.68 (m, 26H), 6.94 (m, 1H), 7.38 (d, J = 8.7 Hz, 1H), 7.51 (m, 1H), 7.87 (d, J = 7.4 Hz, 1H); ^{13}C NMR (101 MHz, D_2O) δ ppm 51.4 (CH_2), 56.6 (CH_2), 58.8 (CH_2), 58.9 (CH_2), 114.2 (C_{Ar}), 114.9 (CH_{Ar}), 120.8 (CH), 121.6 (CH_{Ar}), 122.0 (q, J = 275 Hz, C_q), 126.8 (CH_{Ar}), 138.5 (q, J = 32.2 Hz, C_q), 139.3 (C_{Ar}), 143.9 (C_{Ar}), 162.6 (C_q), 174.1 (C_q), 174.6 (C_q), 180.2 (C_q); ^{19}F NMR (376 MHz, $CDCl_3$) δ ppm −63.4 RP-HPLC t_R = 5.60–9.72 min (16 min method: 0–12 min 10% → 50%); ESI-MS 673.32; HR-ESI-MS obsd 709.1779, 731.1559, calcd 709.1763, 731.1583, [(M + Ca − 3H), M = $C_{28}H_{32}N_6O_{10}F_3$; (M + Ca + Na − 4H), M = $C_{28}H_{35}N_6O_{10}F_3$].

7c. 477 mg (quant.); ^{1}H NMR (400 MHz, D_2O) δ ppm 1.80–4.71 (m, 31H), 7.31 (d, J = 8.6 Hz, 1H), 7.43 (s, 1H), 7.73 (d, J = 8.6 Hz); ^{13}C NMR (101 MHz, D_2O) δ ppm 54.2 (CH_2), 56.6 (CH_2), 58.4 (CH_2), 58.8 (CH_2), 58.9 (CH_2), 70.3 (CH_2), 114.5 (CH_{Ar}), 118.0 (C_{Ar}), 118.3 (CH_{Ar}), 122.0 (CH), 126.0 (CH_{Ar}), 138.3 (C_q), 143.2 (C_{Ar}), 148.8 (C_{Ar}), 164.0 (C_q), 174.1 (C_q), 174.9 (C_q), 180.1 (C_q), 180.2 (C_q); RP-HPLC t_R = 2.95–7.02 min (16 min method: 0–12 min 10% → 50%); ESI-MS obsd 649.29; HR-ESI-MS obsd 685.2175, 707.1980, calcd 685.2152, 707.1971, [(M + Ca − 3H), M = $C_{29}H_{37}N_6O_{11}$; (M + Ca + Na − 4H), M = $C_{29}H_{340}N_6O_{11}$].

7d. 345 mg (quant.); ^{1}H NMR (400 MHz, D_2O) δ ppm 1.11–1.25 (m, 4.19H (3H product, 1.19H EtOH)), 1.73–4.67 (m, 33.8H (33H product, 0.8H EtOH)), 7.32 (d, J = 8.8 Hz, 1H), 7.38–7.45 (m, 1H), 7.83 (d, J = 8.7 Hz, 1H); ^{13}C NMR (101 MHz, D_2O) δ ppm 13.4 (CH_3), 15.1 (CH_3), 32.6 (CH_2), 47.7–48.6 (CH_2), 52.3–53.1 (CH_2), 54.1 (CH_2), 56.6 (CH_2), 58.8 (CH_2), 58.9 (CH_2), 62.3 (CH_2), 114.1 (CH_{Ar}), 120.4 (C_{Ar}), 121.7 (CH_{Ar}), 123.9 (C_q), 137.0 (C_{Ar}), 142.7 (C_{Ar}), 147.7 (C_q), 163.0 (C_q), 173.5 (C_q), 174.0 (C_q), 174.7 (C_q), 180.1 (C_q), 180.2 (C_q); RP-HPLC t_R = 5.70–9.42 min (16 min method: 0–12 min 10% → 50%); ESI-MS obsd 705.32; HR-ESI-MS obsd 741.2431, 763.2234,

calcd 741.2414, 763.2223, [(M + Ca − 3H), M = $C_{32}H_{41}N_6O_{12}$; (M + Ca + Na − 4H), M = $C_{32}H_{44}N_6O_{12}$].

General procedure for Ln complexation. A sample of the ligand (50 mg) was placed into a 4 mL vial equipped with a stirring bar. A 1 : 1 mixture of H_2O and EtOH was added (c = 0.05 M) into the vial using a micropipette, followed by the appropriate (2.4 equiv.) lanthanide salt ($EuCl_3{\cdot}6H_2O$, $TbCl_3$ (anhydrous), or $GdCl_3$ (anhydrous)). The vials were sealed with a screw-cap and parafilm. The mixtures were sonicated to ensure full dissolution. The reaction mixtures were stirred overnight at 45 °C in an alumina bath. The following day the mixture was sonicated again, and then it was transferred dropwise to a 20 mL vial filled with Et_2O. The phases were separated, (the organic phase was removed from the top), and the aqueous layer was loaded onto a silica gel chromatography column (Ø 1 cm, h = 3 cm). Elution with acetonitrile : H_2O (8 : 2 → 6 : 4) yielded the Ln complexes as yellowish-white (ivory) solids. The final products contain a small amount of silica because of the polar conditions applied on the silica column. Most of the residual silica can be removed through membrane filtration (0.2 μm) of the concentrated aqueous solution of the complexes using a syringe. It is important to leave the solution standing for about a day (or at least for several hours) before filtration to allow the silica to precipitate out.

Eu1a. 8 mg (43%); RP-HPLC t_R = 5.85 min (16 min method: 0–8 min: 10 → 20% & 8–12 min: 20% iso); ESI-MS obsd 769.20; HR-ESI-MS obsd 767.15435, calcd 767.15568, [(M − H)$^-$, M = $C_{28}H_{35}N_6O_{10}Eu$].

Gd1a. 10 mg (53%); RP-HPLC t_R = 5.67 min (16 min method: 0–8 min: 10 → 20% & 8–12 min: 20% iso); ESI-MS obsd 774.18; HR-ESI-MS obsd 772.15725, calcd 772.15896, [(M − H)$^-$, M = $C_{28}H_{35}N_6O_{10}Gd$].

Tb1a. 7 mg (37%); RP-HPLC t_R = 5.87 min (16 min method: 0–8 min: 10 → 20% & 8–12 min: 20% iso); ESI-MS obsd 775.30; HR-ESI-MS obsd 773.15826, calcd 773.15953, [(M − H)$^-$, M = $C_{28}H_{35}N_6O_{10}Tb$].

Eu1b. 36 mg (59%); RP-HPLC t_R = 10.80 min (16 min method: 0–8 min: 10 → 20% & 8–12 min: 20% iso); ESI-MS obsd 823.17; HR-ESI-MS obsd 821.12580, calcd 821.12879, [(M − H)$^-$, M = $C_{28}H_{32}N_6O_{10}F_3Eu$].

Gd1b. 35 mg (57%); RP-HPLC t_R = 10.73 min (16 min method: 0–8 min: 10 → 20% & 8–12 min: 20% iso); ESI-MS obsd 828.16; HR-ESI-MS obsd 826.12879, calcd 826.13069, [(M − H)$^-$, M = $C_{28}H_{32}N_6O_{10}F_3Gd$].

Tb1b. 44 mg (71%); RP-HPLC t_R = 10.75 mind (16 min method: 0–8 min: 10 → 20% & 8–12 min: 20% iso); ESI-MS obsd 829.26; HR-ESI-MS obsd 827.12989, calcd 827.13127, [(M − H)$^-$, M = $C_{28}H_{32}N_6O_{10}F_3Tb$].

Eu1c. 52 mg (85%); RP-HPLC t_R = 5.78 min (16 min method: 0–8 min: 10 → 20% & 8–12 min: 20% iso); ESI-MS obsd 799.18; HR-ESI-MS obsd 797.16485, calcd 797.16626, [(M − H)$^-$, M = $C_{29}H_{37}N_6O_{11}Eu$].

Gd1c. 33 mg (53%); RP-HPLC t_R = 5.45 min (16 min method: 0–8 min: 10 → 20% & 8–12 min: 20% iso); ESI-MS obsd 804.26; HR-ESI-MS obsd 802.16777, calcd 802.16956, [(M − H)$^-$, M = $C_{29}H_{37}N_6O_{11}Gd$].

Tb1c. 54 mg (87%); RP-HPLC t_R = 5.43 min (16 min method: 0–8 min: 10 → 20% & 8–12 min: 20% iso); ESI-MS obsd 805.32; HR-ESI-MS obsd 803.16896, calcd 803.17010, [(M − H)$^-$, M = $C_{29}H_{37}N_6O_{11}Tb$].

Eu1d. 35 mg (58%); RP-HPLC t_R = 10.92 min (16 min method: 0–8 min: 10 → 20% & 8–12 min: 20% iso); ESI-MS obsd 855.15; HR-ESI-MS obsd 853.19070, calcd 853.19253, [(M − H)$^-$, M = $C_{32}H_{41}N_6O_{12}Eu$].

Gd1d. 42 mg (69%); RP-HPLC t_R = 10.90 min (16 min method: 0–8 min: 10 → 20% & 8–12 min: 20% iso); ESI-MS obsd 859.76; HR-ESI-MS obsd 802.16777, calcd 802.16956, [(M − H)$^-$, M = $C_{32}H_{41}N_6O_{12}Gd$].

Tb1d. 42 mg (69%); RP-HPLC t_R = 10.87 min (16 min method: 0–8 min: 10 → 20% & 8–12 min: 20% iso); ESI-MS obsd 861.36; HR-ESI-MS obsd 803.16896, calcd 803.17010, [(M − H)$^-$, M = $C_{32}H_{41}N_6O_{12}Tb$].

Conclusions

In conclusion, four new ligands and their Tb, Eu and Gd complexes were synthesised and characterised. The ligands have carbostyril sensitising antennae decorated with 4-Me, 4-CF_3, 4-MOM or 3-CH_2CO_2Et and 4-Me substituents. Antennae are attached to the ligand-binding DOTA framework through a tertiary amide linker, which carries a negatively charged carboxymethyl group. The Tb and Eu complexes had greatly increased quantum yields compared to analogous species wherein the linker was a secondary amide. The increased Φ_{Ln} is due to an enhanced sensitisation efficiency, based on the analysis of the Eu spectra, and, to a much smaller extent, due to a slightly increased intrinsic quantum yield possibly caused by the removal of the amide N–H oscillator from the proximity of the Ln.

The reasons for the improved photophysical properties are likely to be multiple. The blue-shifted antenna triplets should allow for better overlap with the Tb excited states, and thus allow for a more efficient energy transfer. In the case of Eu, a reduction in PeT may contribute; this effect would be smallest for the electron-poor trifluoromethylated antenna. Factors that are difficult to evaluate are: better ISC due to the larger heavy atom effect of the *N*-alkyl group, and the removal of the NH oscillator that may quench the triplet as well as the Ln excited state. Finally, the Ln-antenna distance and orientation may differ in complexes with secondary and with tertiary amide linkers.

Conflicts of interest

There are no conflicts to declare.

Acknowledgements

This work was supported by the Swedish Research Council (project grants 2013-4655 and 2017-04077 to K. E. B.). D. P. is an Erasmus student from the University of Glasgow. We thank

Dr Julien Andres for discussions and critical reading of the manuscript, Michele Bedin for help with the HPLC analysis, and Ashleigh Castner for proofreading.

Notes and references

1 A. de Bettencourt-Dias, in *Luminescence of Lanthanide Ions in Coordination Compounds and Nanomaterials*, John Wiley & Sons Ltd, 2014, pp. 1–48, DOI: 10.1002/9781118682760.ch01.
2 S. J. Butler, M. Delbianco, L. Lamarque, B. K. McMahon, E. R. Neil, R. Pal, D. Parker, J. W. Walton and J. M. Zwier, *Dalton Trans.*, 2015, **44**, 4791–4803.
3 J. M. Zwier, H. Bazin, L. Lamarque and G. Mathis, *Inorg. Chem.*, 2014, **53**, 1854–1866.
4 C. P. Montgomery, B. S. Murray, E. J. New, R. Pal and D. Parker, *Acc. Chem. Res.*, 2009, **42**, 925–937.
5 E. G. Moore, A. P. S. Samuel and K. N. Raymond, *Acc. Chem. Res.*, 2009, **42**, 542–552.
6 M. Sy, A. Nonat, N. Hildebrandt and L. J. Charbonniere, *Chem. Commun.*, 2016, **52**, 5080–5095.
7 S. Petoud, S. M. Cohen, J.-C. G. Buenzli and K. N. Raymond, *J. Am. Chem. Soc.*, 2003, **125**, 13324–13325.
8 C. Y. Chow, S. V. Eliseeva, E. R. Trivedi, T. N. Nguyen, J. W. Kampf, S. Petoud and V. L. Pecoraro, *J. Am. Chem. Soc.*, 2016, **138**, 5100–5109.
9 A. Foucault-Collet, C. M. Shade, I. Nazarenko, S. Petoud and S. V. Eliseeva, *Angew. Chem., Int. Ed.*, 2014, **53**, 2927–2930.
10 E. R. Trivedi, S. V. Eliseeva, J. Jankolovits, M. M. Olmstead, S. Petoud and V. L. Pecoraro, *J. Am. Chem. Soc.*, 2014, **136**, 1526–1534.
11 A. Foucault-Collet, K. A. Gogick, K. A. White, S. Villette, A. Pallier, G. Collet, C. Kieda, T. Li, S. J. Geib, N. L. Rosi and S. Petoud, *Proc. Natl. Acad. Sci. U. S. A.*, 2013, **110**, 17199–17204.
12 A. T. Bui, A. Roux, A. Grichine, A. Duperray, C. Andraud and O. Maury, *Chem. – Eur. J.*, 2018, **24**, 3408–3412.
13 J.-C. G. Bünzli and S. V. Eliseeva, in *Lanthanide Luminescence: Photophysical, Analytical and Biological Aspects*, ed. P. Hänninen and H. Härmä, Springer Berlin Heidelberg, Berlin, Heidelberg, 2011, pp. 1–45, DOI: 10.1007/4243_2010_3.
14 D. Parker, R. S. Dickins, H. Puschmann, C. Crossland and J. A. K. Howard, *Chem. Rev.*, 2002, **102**, 1977–2010.
15 A. Bourdolle, M. Allali, J.-C. Mulatier, B. Le Guennic, J. M. Zwier, P. L. Baldeck, J.-C. G. Bunzli, C. Andraud, L. Lamarque and O. Maury, *Inorg. Chem.*, 2011, **50**, 4987–4999.
16 R. M. Supkowski and W. D. Horrocks Jr., *Inorg. Chim. Acta*, 2002, **340**, 44–48.
17 A. Beeby, I. M. Clarkson, R. S. Dickins, S. Faulkner, D. Parker, L. Royle, S. A. S. de, J. A. G. Williams and M. Woods, *J. Chem. Soc., Perkin Trans. 2*, 1999, 493–504, DOI: 10.1039/a808692c.
18 C. Doffek, N. Alzakhem, M. Molon and M. Seitz, *Inorg. Chem.*, 2012, **51**, 4539–4545.
19 C. Doffek, N. Alzakhem, C. Bischof, J. Wahsner, T. Gueden-Silber, J. Luegger, C. Platas-Iglesias and M. Seitz, *J. Am. Chem. Soc.*, 2012, **134**, 16413–16423.
20 D. Parker and J. A. G. Williams, *J. Chem. Soc., Perkin Trans. 2*, 1996, 1581–1586, DOI: 10.1039/p29960001581.
21 D. Parker, P. K. Senanayake and J. A. G. Williams, *J. Chem. Soc., Perkin Trans. 2*, 1998, 2129–2139.
22 D. Parker, *Coord. Chem. Rev.*, 2000, **205**, 109–130.
23 G.-L. Law, R. Pal, L. O. Palsson, D. Parker and K.-L. Wong, *Chem. Commun.*, 2009, 7321–7323, DOI: 10.1039/B920222F.
24 R. A. Poole, C. P. Montgomery, E. J. New, A. Congreve, D. Parker and M. Botta, *Org. Biomol. Chem.*, 2007, **5**, 2055–2062.
25 F. Kielar, C. P. Montgomery, E. J. New, D. Parker, R. A. Poole, S. L. Richardson and P. A. Stenson, *Org. Biomol. Chem.*, 2007, **5**, 2975–2982.
26 T. J. Soerensen, A. M. Kenwright and S. Faulkner, *Chem. Sci.*, 2015, **6**, 2054–2059.
27 A. Watkis, R. Hueting, T. J. Soerensen, M. Tropiano and S. Faulkner, *Chem. Commun.*, 2015, **51**, 15633–15636.
28 J. Lehr, M. Tropiano, P. D. Beer, S. Faulkner and J. J. Davis, *Chem. Commun.*, 2015, **51**, 15944–15947.
29 W. J. Evans, J. L. Shreeve, J. W. Ziller and R. J. Doedens, *Inorg. Chem.*, 1995, **34**, 576–585.
30 P. R. Selvin and J. E. Hearst, *Proc. Natl. Acad. Sci. U. S. A.*, 1994, **91**, 10024–10028.
31 A. Cha, G. E. Snyder, P. R. Selvin and F. Bezanilla, *Nature*, 1999, **402**, 809–813.
32 P. Ge and P. R. Selvin, *Bioconjugate Chem.*, 2004, **15**, 1088–1094.
33 H. E. Rajapakse, D. R. Reddy, S. Mohandessi, N. G. Butlin and L. W. Miller, *Angew. Chem., Int. Ed.*, 2009, **48**, 4990–4992.
34 A. Mohamadi and L. W. Miller, *Bioconjugate Chem.*, 2016, **27**, 2540–2548.
35 M. Rajendran, E. Yapici and L. W. Miller, *Inorg. Chem.*, 2014, **53**, 1839–1853.
36 D. R. Reddy, L. E. Pedro Rosa and L. W. Miller, *Bioconjugate Chem.*, 2011, **22**, 1402–1409.
37 A. M. Reynolds, B. R. Sculimbrene and B. Imperiali, *Bioconjugate Chem.*, 2008, **19**, 588–591.
38 M. S. Tremblay, M. Halim and D. Sames, *J. Am. Chem. Soc.*, 2007, **129**, 7570–7577.
39 D. Kovacs, X. Lu, L. S. Mészáros, M. Ott, J. Andres and K. E. Borbas, *J. Am. Chem. Soc.*, 2017, **139**, 5756–5767.
40 H.-K. Lee, H. Cao and T. M. Rana, *J. Comb. Chem.*, 2005, **7**, 279–284.
41 D. Kovacs and K. E. Borbas, *Coord. Chem. Rev.*, 2018, **364**, 1–9.
42 O. V. Dolomanov, L. J. Bourhis, R. J. Gildea, J. A. K. Howard and H. Puschmann, *J. Appl. Crystallogr.*, 2009, **42**, 339–341.

43 G. Saroja, N. B. Sankaran and A. Samanta, *Chem. Phys. Lett.*, 1996, **249**, 392–398.
44 M. Latva, H. Takalo, V.-M. Mukkala, C. Matachescu, J. C. Rodriguez-Ubis and J. Kankare, *J. Lumin.*, 1997, **75**, 149–169.
45 M. H. V. Werts, R. T. F. Jukes and J. W. Verhoeven, *Phys. Chem. Chem. Phys.*, 2002, **4**, 1542–1548.
46 B. M. Reddy, B. Thirupathi and M. K. Patil, *Open Catal. J.*, 2009, **2**, 33–39.
47 I. Sosic, M. Gobec, B. Brus, D. Knez, M. Zivec, J. Konc, S. Lesnik, M. Ogrizek, A. Obreza, D. Zigon, D. Janezic, I. Mlinaric-Rascan and S. Gobec, *Angew. Chem., Int. Ed.*, 2016, **55**, 5745–5748.
48 G. Sheldrick, *Acta Crystallogr., Sect. C: Struct. Chem.*, 2015, **71**, 3–8.